JCTC Journal of Chemical Theory and Computation

Development of OPLS-AA Force Field Parameters for 68 Unique Ionic Liquids

Somisetti V. Sambasivarao and Orlando Acevedo*

Department of Chemistry and Biochemistry, Auburn University, Auburn, Alabama 36849

Received January 6, 2009

Abstract: OPLS-AA force field parameters have been developed and validated for use in the simulation of 68 unique combinations of room temperature ionic liquids featuring 1-alkyl-3-methylimidazolium [RMIM] (R = Me, Et, Bu, Hex, Oct), *N*-alkylpyridinium [RPyr], and choline cations, along with Cl^-, PF_6^-, BF_4^-, NO_3^-, $AlCl_4^-$, $Al_2Cl_7^-$, TfO^-, saccharinate, and acesulfamate anions. The new parameters were fit to conformational profiles from gas-phase ab initio calculations at the LMP2/cc-pVTZ(-f)//HF/6−31G(d) theory level and compared to experimental condensed-phase structural and thermodynamic data. Monte Carlo simulations of the ionic liquids gave relative deviations from experimental densities of ca. 1−3% at 25 °C for most combinations and also yielded close agreement over a temperature range of 5 to 90 °C. Predicted heats of vaporization compared well with available experimental data and estimates. Transferability of the new parameters to multiple alkyl side-chain lengths for [RMIM] and [RPyr] was determined to give excellent agreement with charges and torsion potentials developed specific to desired alkyl lengths in 35 separate ionic liquid simulations. As further validation of the newly developed parameters, the Kemp elimination reaction of benzisoxazole via piperidine was computed in 1-butyl-3-methylimidazolium hexafluorophosphate [BMIM][PF_6] using mixed quantum and molecular mechanics (QM/MM) simulations and was found to give close agreement with the experimental free energy of activation.

Introduction

Ionic liquids are a unique class of solvent, generally defined as a material containing only ionic species with a melting point below 100 °C.[1,2] These "designer" solvents are typically composed of a low symmetry organic cation, such as the well-recognized 1-alkyl-3-methylimidazolium [RMIM] and *N*-alkylpyridinium [RPyr] cation classes, and a weakly coordinating inorganic or organic anion with a diffuse negative charge like hexafluorophosphate [PF_6] or tetrafluoroborate [BF_4].[3] Ion components can be fine-tuned through different functional groups to enhance the degree of localized structuring in the liquid phase, which distinguishes ionic liquids from molecular solvents and solutions containing dissociated ions.[4] This distinctive structural behavior[5] in conjunction with their attractive properties, e.g., low viscosities, negligible vapor pressure, and excellent thermal and chemical stabilities, has led to numerous advances in electrochemistry,[6] separation science,[7] catalysis,[8−10] organic synthesis,[11] materials,[12] and applications with lanthanides and actinides.[13]

Ionic liquids are often touted as green alternatives to volatile organic solvents. However, their potential impact on the environment is strongly dictated by ionic liquid selection.[9,14,15] For example, toxicity testing of 1-butyl-3-methylimidazolium [BMIM] and *N*-1-butylpyridinium [BPyr] on *Daphnia magna*, a common fresh water crustacean and aquatic food-chain base, found the cations to be half as toxic as toluene (EC_{50} of ca. 20 mg/L) and increasing the alkyl chain length to dodecyl increased the ecotoxicity by a factor of 2500 (EC_{50} of 4 μg/L).[15] In addition, combinations of [BMIM] with [BF_4] or [PF_6] anions have been determined to possess a negligible biodegradability,[16] allowing for their persistence in the environment for a considerable length of time. More environmentally friendly ionic liquids have

* E-mail: orlando.acevedo@auburn.edu.

10.1021/ct900009a CCC: $40.75
Published on Web 03/12/2009

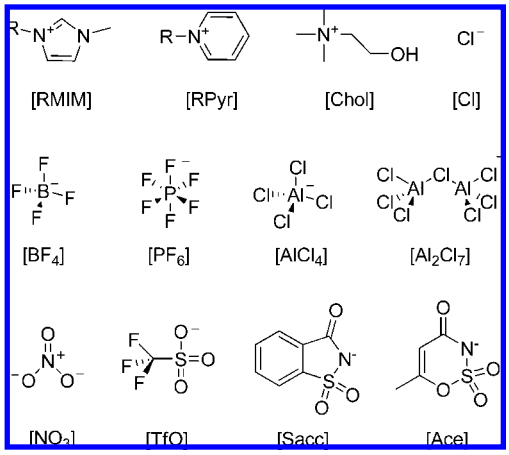

Figure 1. Ionic liquid-forming ions. R = M (methyl), E (ethyl), B (butyl), H (hexyl), and O (octyl).

recently been explored based on the choline cation [Chol],[17] a food-grade additive, and imidazolium derivatives designed for biodegradability[18] in combination with anions based on amino acids,[19] saccharinate [Sacc],[17] and acesulfamate [Ace][17,20] ([Sacc] and [Ace] are used as artificial sweeteners).

This study seeks to develop force field potentials for the atomistic simulation of both widely used ionic liquid combinations and next-generation alternatives with smaller environmental impact. In this respect, OPLS-AA parameters have been created and validated for use in the simulation of 68 unique combinations of room temperature ionic liquids featuring [RMIM] (R = Me, Et, Bu, Hex, Oct), [RPyr], and [Chol] cations, along with [PF_6], [BF_4], [Sacc], [Ace], nitrate [NO_3], chloride [Cl], tetrachloroaluminate [$AlCl_4$], heptachlorodialuminate [Al_2Cl_7], and triflate [TfO] anions (Figure 1). Many of the ions presented in this work have already been featured in other molecular dynamics[21−24] and Monte Carlo[25] studies for a variety of force fields, e.g., CHARMM,[26] AMBER,[27] and OPLS-AA.[28] Therefore it is important to stress that in addition to the parametrization of previously unpublished ionic liquids, e.g., [Chol], [Sacc], and [Ace], this study explored an unprecedented number of cation/anion combinations with two completely different charge and torsion sets for a detailed comparison of parameter transferability. The first charge/torsion set is potentially transferable to any alkyl side-chain length on the [RMIM] and [RPyr] cations (tested up to R = octyl) and the second set is specific to the ionic liquid cations: [EMIM], [BMIM], [MPyr], [EPyr], and [BPyr]. In addition, the current work validated the parameters for temperatures ranging from 5 to 90 °C against experimental densities for 11 unique ionic liquid combinations; most previous work focused on room temperature.

Monte Carlo (MC) simulations of the ionic liquid parameters gave predicted densities and heats of vaporization, ΔH_{vap}, in close agreement with experimentally observed values. The driving force behind the newly developed parameter set is to produce a computationally accurate representation of the reaction medium for use in mixed quantum and molecular mechanics (QM/MM) calculations. The objective is to understand the microscopic details on how ionic liquids influence chemical reactions accelerated and controlled by different cation and anion combinations.[8,9] Our recent work on Diels−Alder reactions in the chloroaluminate ionic liquids [EMIM][$AlCl_4$] and [EMIM][Al_2Cl_7] emphasized the importance of intermolecular interactions on the rate of reaction.[25] In this study, the Kemp elimination ring-opening of benzisoxazole in [BMIM][PF_6] using piperidine as the base has been carried out using QM/MM calculations and was found to give good agreement with the experimental free energy of activation.

Computational Methods

OPLS-AA Force Field. The OPLS-AA force field[28] formalism was chosen to represent the ionic liquids. As a brief overview, the total energy of the ionic systems are evaluated as a sum of individual energies for the harmonic bond stretching and angle bending terms, a Fourier series for torsional energetics, and Coulomb and 12−6 Lennard−Jones terms for the nonbonded interactions, see eqs 1−4. The parameters are the force constants k, the r_o and θ_o reference values, the Fourier coefficients V, the partial atomic charges, q, and the Lennard−Jones radii and well depths, σ and ε.

$$E_{\text{bonds}} = \sum_i k_{b,i}(r_i - r_{o,i})^2 \quad (1)$$

$$E_{\text{angles}} = \sum_i k_{b,i}(\theta_i - \theta_{o,i})^2 \quad (2)$$

$$E_{\text{torsion}} = \sum_i \left[\frac{1}{2}V_{1,i}(1 + \cos\varphi_i) + \frac{1}{2}V_{2,i}(1 + \cos 2\varphi_i) + \frac{1}{2}V_{3,i}(1 + \cos 3\varphi_i) + \frac{1}{2}V_{4,i}(1 + \cos 4\varphi_i)\right] \quad (3)$$

$$E_{\text{nonbond}} = \sum_i \sum_{j>i} \left\{\frac{q_i q_j e^2}{r_{ij}} + 4\varepsilon_{ij}\left[\left(\frac{\sigma_{ij}}{r_{ij}}\right)^{12} - \left(\frac{\sigma_{ij}}{r_{ij}}\right)^{6}\right]\right\} \quad (4)$$

The geometric combining rules regularly used for the Lennard−Jones coefficients are employed: $\sigma_{ij} = (\sigma_{ii}\sigma_{jj})^{1/2}$ and $\varepsilon_{ij} = (\varepsilon_{ii}\varepsilon_{jj})^{1/2}$.[28] Nonbonded interactions are evaluated intermolecularly and for intramolecular atom pairs separated by three or more bonds. In order to use identical parameters for both intra- and intermolecular interactions the 1,4-intramolecular interactions are reduced by a factor of 2.[28] To retain compatibility with OPLS-AA, all present parameters were developed in a similar fashion to recent parametrization efforts by Jorgensen and co-workers.[29−31] Whenever appropriate, published potentials were retained without change. This includes assigning all standard bond stretching and angle bending force constants from OPLS-AA, which may also include some entries from the AMBER-AA force field.[27] All Lennard−Jones parameters also came from the OPLS-AA parameter set except when explicitly stated. The present work then focused on the development of Fourier coefficients, partial charges, and equilibrium geometries, and the validation of multiple ionic liquid combinations.

Ab Initio Calculations. All individual ions, i.e., [RMIM] (R = Me, Et, Bu), [RPyr] (R = Me, Et, Bu), and [Chol] cations with [Cl], [PF_6], [BF_4], [NO_3], [$AlCl_4$], [Al_2Cl_7],

[TfO], [Sacc], and [Ace] anions, were optimized using the Jaguar program[32] at the Hartree−Fock (HF) theory level using the 6−31G(d) basis set with subsequent single-point energy calculations using the local MØller−Plesset second-order perturbation (LMP2)[33] method and the correlation-consistent polarized valence cc-pVTZ(-f) basis set.[34] This LMP2/cc-pVTZ(-f)//HF/6−31G(d) method is the current practice for OPLS-AA parametrization.[31] Vibrational analytical frequency calculations at the HF/6−31G(d) were carried out to confirm all minima as stationary points. The ab initio derived ion geometries were used for the equilibrium bond and angle, r_o and θ_o, reference values in the force field and given in the Supporting Information. Partial charges were computed by fitting the molecular electrostatic potential (ESP) at the atomic centers. For a better description of the charge density, LMP2 dipole moments were also computed along with a coupled perturbed Hartree−Fock (CPHF) term. Charges were symmetrized for similar atoms and used for the Coulombic nonbonded force field partial charges. Torsional energies were fit to reproduce computed LMP2/cc-pVTZ(-f)//HF/6−31G(d) energy scans. Calculations at this level have been reported to yield highly accurate conformational energies with average errors of ca. 0.25 kcal/mol for reported test sets and 0.6 kcal/mol for perfluorolalkanes.[31] Greater detail on the torsional scans and assignment of partial charges are given in Results and Discussion.

Ionic Liquid Simulations. The Metropolis Monte Carlo (MC) simulations were performed with the BOSS 4.6 program.[35] All cations were fully flexible, i.e., all bond stretching, angle bending, and torsional motions were sampled. Anions were simulated as rigid molecules, and as a result no additional intramolecular anion parametrization was necessary. The use of rigid anions in OPLS-AA has been shown to provide an accurate representation of ionic liquid physical properties,[23] including use as a reaction medium for a computed QM/MM Diels−Alder reaction study.[25] Periodic boundary conditions have been applied to boxes containing 190 ion pairs with long-range interactions handled with Ewald summations. In short, Ewald summations calculate the exact electrostatic energy of an infinite lattice of identical copies of the simulation cell. This suppresses artifacts resulting from the simple cutoff of the long-range electrostatic interactions prevalent in the ionic liquid. The liquid-phase simulations were carried out by placing the 380 ions at random positions in the simulation box (see Figure 2), and a temperature value of 1000 °C was initially applied for 10 million configurations in the NVT ensemble to encourage a thorough mixing. The simulations were then equilibrated at 25 °C for 100−200 million MC steps in the NPT ensemble. The heating/NVT and equilibration/NPT simulations on each ionic liquid system were repeated sequentially an average of 4−6 times until the energy and volume of the system no longer decreased. A pressure of 1 atm was used in all cases. The computed densities, heats of vaporization, energy distributions, and conformational properties were very well converged with MC simulations of this length.

In order to compute the heats of vaporization, ΔH_{vap}, MC simulations needed to be performed on the gas-phase ion pair of the corresponding ionic liquid because of the flexibility of the cations. Experimental evidence suggests that ionic liquids go into the vapor phase in ion pairs.[36] Gas-phase simulations consisted of 1 million configurations of equilibration, followed by 2 million configurations of averaging. For the liquids, the systems were periodic and tetragonal with $c/a = 1.5$; as an example, a is ca. 34.3 and 35.5 Å for [BMIM][BF_4] and [BMIM][PF_6] (box sizes for all ionic liquids are given in the Supporting Information).

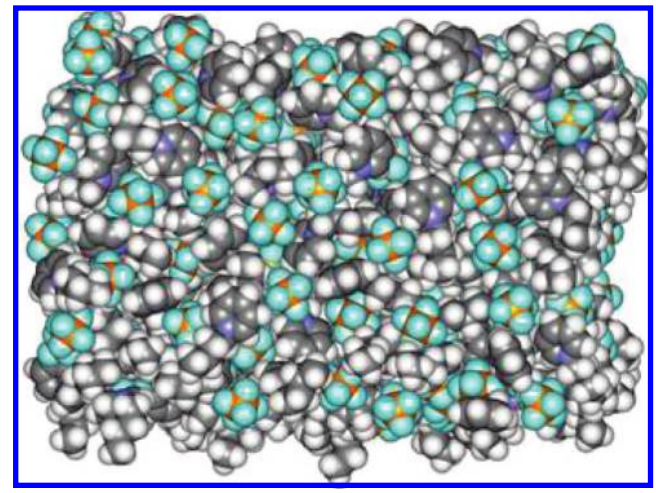

Figure 2. Illustration of an equilibrated [BPyr][PF_6] ionic liquid simulation box.

Solvent−solvent intermolecular cutoff distances of 12 Å were employed for the tail carbon atom of each side chain (methyl and alkyl), a midpoint carbon on the alkyl chain, and the ring carbon between both nitrogens for imidazolium. Cutoff atoms were also based on alkyl side-chain length for *N*-pyridinium using the carbon at the end of the alkyl chain, a midpoint carbon on the side chain, the nitrogen atom, and the carbon ring atom para to the nitrogen. For choline, atoms O and N, along with two Cs bonded to N (methyl and on the chain) were used for cutoffs. Center atoms, e.g., B in BF_4^- and P in PF_6^-, were used for the anions. If any distance is within the cutoff, the entire solvent−solvent interaction was included. Adjustments to the allowed ranges for rotations, translations, and dihedral angle movements led to overall acceptance rates of about 40−50% for new configurations. The ranges for bond stretching and angle bending were set automatically by the BOSS program on the basis of force constants and temperature. All MC calculations were run on a Linux cluster at Auburn University, and all ab initio calculations were performed on computers located at the Alabama Supercomputer Center.

Results and Discussion

Partial Charges. Ab initio calculations at the LMP2/cc-pVTZ(-f)//HF/6−31G(d) theory level were carried out on the isolated gas-phase ions in order to facilitate the transferability of the charge model to multiple ionic liquid combinations. All anions were geometry optimized, and Coulombic charges were assigned from the ESP fits (Table 1). For the cations, multiple low-energy geometry configurations exist stemming primarily from torsion rotations, i.e., the alkyl side

Table 1. Nonbonded Parameters for [Cl], [PF_6], [BF_4], [NO_3], [$AlCl_4$], [Al_2Cl_7], [TfO], Saccharinate [Sac], and Acesulfamate [Ace] Anions[a]

anion	atom type	q (e)	σ (Å)	ε (kcal mol^{-1})
[Cl][b]	Cl	−1.00	3.770	0.148
[BF_4][c]	B	0.8276	3.5814	0.095
	F	−0.4569	3.1181	0.060
[PF_6]	P	1.3400	3.740	0.200
	F	−0.3900	3.1181	0.061
[NO_3]	N	0.794	3.150	0.170
	O	−0.598	2.860	0.210
[$AlCl_4$][d]	Al	0.6452	4.050	0.100
	Cl	−0.4113	3.770	0.148
[Al_2Cl_7][d]	Al	0.5455	4.050	0.100
	ClM[e]	−0.1404	3.770	0.148
	Cl	−0.3251	3.770	0.148
[TfO]	S	1.1887	3.550	0.250
	O	−0.6556	2.960	0.210
	C	0.2692	3.500	0.066
	F	−0.1637	2.950	0.053
[Sac]	C1	−0.0519	3.550	0.070
	C2	−0.1882	3.550	0.070
	C3	−0.0235	3.550	0.070
	C4	−0.2759	3.550	0.070
	C5	0.1293	3.550	0.070
	C6	−0.1968	3.550	0.070
	C9	0.5502	3.750	0.105
	S7	1.2149	3.550	0.250
	N8	−0.6889	3.250	0.170
	OC	−0.5950	2.960	0.210
	OS	−0.6285	2.960	0.210
	HA	0.1132	2.420	0.030
	HB	0.0782	2.420	0.030
[Ace]	C1	−0.8536	3.550	0.070
	C2	0.6670	3.550	0.070
	C6	0.9507	3.750	0.105
	C7	−0.3083	3.500	0.066
	O3	−0.5087	2.900	0.140
	OB	−0.6573	2.960	0.210
	OS	−0.6158	2.960	0.170
	S4	1.3355	3.550	0.250
	N5	−0.8224	3.250	0.170
	HA	0.0666	2.500	0.030
	HB	0.2289	2.420	0.030

[a] All Lennard−Jones (LJ) nonbonded parameters are from the OPLS-AA force field unless otherwise stated. Atom types for [Sacc] and [Ace] are shown in Figure 4. [b] LJ parameter for Cl taken from ref 23. [c] LJ parameter for B taken from ref 24. [d] LJ parameters taken from refs 24 and 25. [e] Corresponds to Cl atom bridging the Al atoms.

chains in the [RMIM] and [RPyr] ions and choline's internal N−C−C−O dihedral. This presented the challenge of developing a single set of charges per cation family that could accurately represent different alkyl lengths and orientations. ESP charges were initially computed for all available [RMIM] and [RPyr] energy-minimized stationary points, where R = Me, Et, and Bu. An average partial charge value for each atom in [RMIM] and [RPyr] was developed by appropriately weighting the contribution of each ground-state structure to the overall conformational population. For example, the partial charges specific to [BMIM] (see values in Figure 3) were computed from a two-state model and the Boltzmann distribution based on gauche and trans side-chain optimized energies for the cation. Charges specific to [EMIM], [MPyr], and [EPyr] are given in the Supporting Information. To assign a final charge set to [RMIM], all charges for [MMIM], [EMIM], and [BMIM] were appropriately weighted and averaged (see Table 2 and Figure 3). For the ring atoms, e.g., NA, CW, HW in [RMIM], departures in charge from symmetry were small in the R = Me, Et, and Bu ions; hence, the atoms were given symmetrical values to facilitate transferability. Charges for the carbon and hydrogen atoms, CS and HS, present in the middle of the alkyl side chains (-CH_2-) were taken directly from OPLS-AA alkane values[28] to allow the simulation of any [RMIM] desired chain length (tested up to octyl in the present work). In the simulations of [MMIM], the CM and HM atom types are used in both methyl groups attached to the 1 and 3 nitrogen positions of the imidazolium. A set of transferable charges for [RPyr] and a specific set for choline were computed in an identical fashion (Table 2).

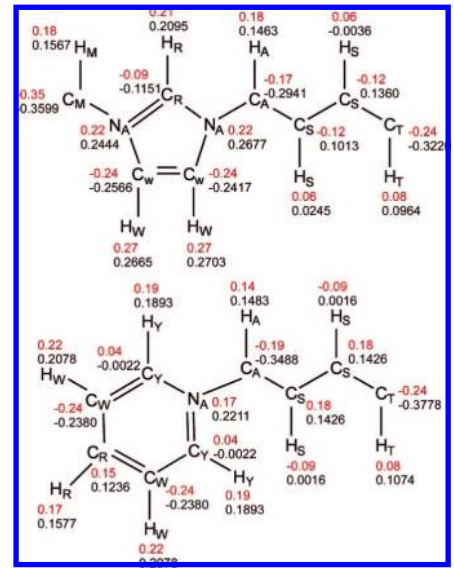

Figure 3. Partial charges assigned for atom types in [RMIM] and [RPyr] in red, and charges exclusively for use in [BMIM] and [BPyr] in black.

The use of averaged point charges was necessary for a fully transferable force field; however, a direct comparison of the accuracy between these [RMIM] and [RPyr] charges versus point charges specific to [EMIM], [BMIM], [MPyr], [EPyr], and [BPyr] was evaluated in this study. Thirty-five ionic liquid combinations were computed using both charge sets, along with the appropriate torsion terms, to compare differences in predicted densities and heats of vaporization for a quantitative evaluation of the final charges presented in Table 2. Most Lennard−Jones (LJ) parameters were taken directly from the OPLS-AA force field; for example, parameters for [RMIM] and [RPyr] were based on imidazole[37] and pyridine,[38] respectively. However, any LJ parameters not assigned from OPLS-AA are specified in Table 1.

Intramolecular Potentials. The resultant geometries from the ab initio calculations were used to obtain the equilibrium bond and angle reference values, r_o and θ_o, for the simulations; the final values are given in the Supporting Information. To allow full flexibility for the cations, appropriate bond and angle force constants, and Fourier coefficients for ring atoms on [RMIM] and [RPyr] were taken directly from published OPLS-AA parameters.[22,37,38] In this work, new

Table 2. Nonbonded Parameters for 1-Alkyl-3-methylimidazolium [RMIM], *N*-Alkylpyridinium [RPyr], and Choline [Chol] Cations[a]

cation	atom type	q (e)	σ (Å)	ε (kcal mol^{-1})
[RMIM]	CR	−0.09	3.55	0.070
	NA	0.22	3.25	0.170
	CW	−0.24	3.55	0.070
	CM	−0.35	3.50	0.066
	CA	−0.17	3.50	0.066
	CS	−0.12	3.50	0.066
	CT	−0.24	3.50	0.066
	HR	0.21	2.42	0.030
	HW	0.27	2.42	0.030
	HM	0.18	2.50	0.030
	HA	0.18	2.50	0.030
	HS	0.06	2.50	0.030
	HT	0.08	2.50	0.030
[RPyr]	CR	0.15	3.55	0.070
	CW	−0.24	3.55	0.070
	CY	0.04	3.55	0.070
	NA	0.17	3.25	0.170
	CM	−0.39	3.50	0.066
	CA	−0.19	3.50	0.066
	CS	0.18	3.50	0.066
	CT	−0.24	3.50	0.066
	HR	0.17	2.42	0.030
	HW	0.22	2.42	0.030
	HY	0.19	2.42	0.030
	HM	0.16	2.50	0.030
	HA	0.14	2.50	0.030
	HS	−0.09	2.50	0.030
	HT	0.08	2.50	0.030
[Chol]	NA	0.1640	3.250	0.170
	CA	−0.3847	3.500	0.066
	CS	−0.1111	3.500	0.066
	CW	0.2318	3.500	0.066
	OY	−0.6547	3.070	0.170
	HA	0.1934	2.500	0.030
	HS	0.1251	2.500	0.030
	HW	0.0398	2.500	0.030
	HY	0.4537	0.000	0.000

[a] Atom types for [RMIM], [RPyr], and [Chol] are given in Figures 3 and 4.

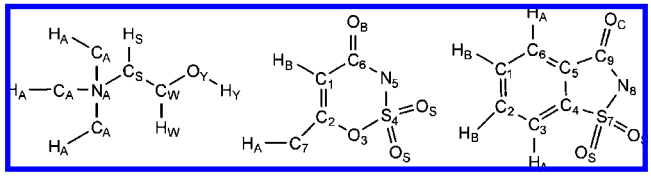

Figure 4. Atom types for choline [Chol], acesulfamate [Ace], and saccharinate [Sacc].

Fourier coefficients for the alkyl side chains of [RMIM] and [RPyr] and an entire new set for the choline cation were developed to reproduce all possible rotations. Vibrational frequencies as is typical of the OPLS force field were not parametrized and will require further refinement of the force constants if greater accuracy is desired. The focus of the ionic liquid OPLS-AA parameter set is to accurately reproduce intermolecular interactions such as density and thermodynamic quantities such as the heats of vaporization.

Torsions. The procedure for establishing the missing Fourier coefficients involved direct adjustment of the OPLS-AA torsional parameters to reproduce the energy differences between conformational energy minima from ab initio calculations. For each dihedral angle, energy profiles were

Table 3. Torsional Fourier Coefficients (kcal/mol) for 1-Alkyl-3-methylimidazolium [RMIM] and Specific to [EMIM] and [BMIM] Charge Sets

torsion	V_1	V_2	V_3	cation
NA-CA-CT-HT	0.000	0.000	0.000	[RMIM]
	0.000	0.000	0.350	[EMIM]
CW-NA-CA-CT	−4.355	−4.575	−1.375	[RMIM]
	−0.599	−1.750	0.290	[EMIM]
CR-NA-CA-CT	−2.000	−0.275	−1.650	[RMIM]
	−0.555	0.479	0.200	[EMIM]
CW-NA-CA-HA	−2.700	−5.650	0.355	[RMIM]
	−0.755	−2.125	0.400	[EMIM]
	−1.400	−2.650	0.175	[BMIM]
CW-NA-CA-CS	−2.110	−5.000	0.345	[RMIM]
	−1.910	−1.500	0.290	[BMIM]
CR-NA-CA-CS	−0.159	0.095	−0.010	[RMIM]
	−1.659	−0.555	−0.375	[BMIM]
NA-CA-CS-CS	−0.788	0.800	0.400	[RMIM]
	−1.788	0.756	−0.288	[BMIM]
HA-CA-CS-HS	0.000	−0.150	0.518	[RMIM]
	0.000	0.000	0.318	[BMIM]

Table 4. Torsional Fourier Coefficients (kcal/mol) for *N*-Alkylpyridinium [RPyr] and Specific to [EPyr] and [BPyr] Charge Sets

torsion	V_1	V_2	V_3	cation
CY-NA-CA-CT	0.000	0.010	0.000	[RPyr]
	0.000	0.150	0.000	[EPyr]
NA-CA-CT-HT	0.000	0.000	0.020	[RPyr]
	0.000	0.000	0.400	[EPyr]
HA-CA-CT-HT	0.000	0.000	0.518	[RPyr]
	0.000	0.000	0.332	[EPyr]
NA-CA-CS-HS	0.000	0.000	0.200	[RPyr]
	−0.700	−0.500	0.000	[BPyr]
HA-CA-CS-HS	0.000	0.000	0.418	[RPyr]
	−1.700	−1.710	0.655	[BPyr]
CY-NA-CA-CS	0.000	−0.050	−0.200	[RPyr]
	0.000	0.180	0.000	[BPyr]
NA-CA-CS-CS	−0.788	0.400	−0.288	[RPyr]
	−0.233	1.400	−0.290	[BPyr]

obtained by rotating the [RMIM] and [RPyr] alkyl side chains and all available [Chol] dihedrals in increments of 15° for each ion with a constrained minimization carried out using the LMP2/cc-pVTZ(-f)//HF/6−31G(d) theory level. Only the dihedrals involved in the torsional potential energy surface were restrained; the remainder of the ion was fully flexible. Each [MMIM], [EMIM], [BMIM], [MPyr], [EPyr], [BPyr], and [Chol] cation was individually parametrized using their specific charge set with coefficients, V_1 to V_3, that gave the best overall fit for all rotatable bonds (Tables 3−5). The resultant Fourier coefficients were then refitted to give the best overall values for the general [RMIM] and [RPyr] cation families, taking into account the general atomic charge sets.

As an example, the energy profiles for the CT-CA-NA-CW/Y and HT-CT-CA-NA rotations in [EMIM] and [EPyr] using the fully transferable parameters (in blue) and the parameters specific to the individual cations (in green) are given in Figure 5; LMP2/cc-pVTZ(-f)//HF/6−31G(d) energy values are presented in black along with the original OPLS-AA parameters in red. Positions of all the minima and maxima were shifted to achieve the lowest possible rms energy error with respect to the quantum mechanical results. The specific charge/torsion parameter sets for the individual

Table 5. Torsional Fourier Coefficients (kcal/mol) for Choline [Chol]

torsion	V_1	V_2	V_3
CW-CS-NA-CA	0.100	0.550	0.650
CA-NA-CA-HA	0.000	0.000	0.825
CS-NA-CA-HA	0.000	0.000	0.940
HS-CS-NA-CA	0.000	1.000	0.700
OY-CW-CS-NA	−6.000	−5.000	3.200
OY-CW-CS-HS	−0.500	−2.500	0.250
HW-CW-CS-NA	−6.000	−7.000	0.750
HW-CW-CS-HS	6.000	−3.000	2.000
HY-OY-CW-CS	−0.356	−0.174	0.350
HY-OY-CW-HW	−3.000	1.000	−2.000
X-NA-X-X[a]	0.000	2.000	0.000

[a] Improper torsion.

cations typically performed better than the generalized parameter set, e.g., the HT-CT-CA-NA rotation in [EMIM] (Figure 5). However, energy profiles for the dihedral rotations were considerably improved using both parameter sets when compared to the unaltered OPLS-AA potentials. The highly transferable [RMIM] and [RPyr] general parameter set enabled most dihedral rotations to be appropriately modeled with good accuracy (multiple energy profiles for [RMIM] and [RPyr] given in the Supporting Information (Figures S3−S10). For example, the energy barriers for dihedral rotations in the 1-propyl-3-methylimidazolium [PMIM] and *N*-1-propylpyridinium [PPyr] cations were well reproduced when using the general [RMIM] and [RPyr] parameter sets despite not being specifically taken into consideration during the parametrization process (Figures S4 and S7). In addition, the simulation of longer alkyl side chains, such as hexyl and octyl, using the [RMIM] and [RPyr] general parameters also gave good agreement with experimental densities and heats of vaporization data, as discussed below.

Density. With satisfactory agreement achieved between the newly developed OPLS-AA parameters and the ab initio calculations for the ionic structures, subsequent MC simulations for 68 unique ionic liquid combinations were carried out. The systems were composed of 190 ion pairs at 25 °C and 1 atm. Each simulation required over 500 million MC configurations to properly equilibrate the periodic boxes using Ewald summations. The computed densities for the solvents are given in Tables 6−8. The imidazolium-based ionic liquids provided the largest amount of experimental data to validate the newly developed force field (Figures 6 and 7). However, in many cases, different experimental measurements varied by as much as 5% per solvent (Table 6). Relative deviations from experimental density values were ca. 1−3% for most [RMIM] ionic liquid combinations using both the fully transferable OPLS-AA force field and the parameters developed specifically for [EMIM] and [BMIM]. The limited amount of reported densities for the [RPyr][BF_4] ionic liquids also compared well with the simulations (Table 7).

Chloroaluminate-based ionic liquids gave slightly larger deviations at ca. 4−5%. Exact agreement could not be expected because the ionic composition of the experimental and modeled systems is not identical. For example, Raman,[39] ^{27}Al NMR,[40] and mass spectra[41] all indicate that when $AlCl_3$ comprises <50% mol of the [EMIM][Cl] ionic liquid melt, [$AlCl_4$] is the only chloroaluminate species present along with chloride ions that are not bound to aluminum. A ratio greater than 1:1 $AlCl_3$-to-[EMIM][Cl] gives [$AlCl_4$] and [Al_2Cl_7] as the principal anionic constituents of the melt from ^{27}Al NMR[42] and negative-ion FAB mass spectra.[43] Despite underestimation of the densities, the simulations for [RMIM]-[$AlCl_4$] and [RMIM][Al_2Cl_7] reproduced the relative trend of decreasing density with increasing alkyl chain length. In addition, the computed heats of vaporization are strikingly similar to the experimental values for [BMIM][$AlCl_4$] and [HMIM][$AlCl_4$] (Table 6). The OPLS-AA chloroaluminate solvents have previously provided an appropriate reaction medium environment for the Diels−Alder reaction using QM/MM methodology.[25]

The errors in the densities computed for choline-based ionic liquids were significantly larger (see Table 8) despite using the same parametrization procedure as the [RMIM]- and [RPyr]-based ionic liquids. For example, simulation of [Chol][Sacc] gave a predicted density of 1.200 g/cm^3 compared to 1.383 g/cm^3 experimentally and [Chol][Ace] gave a calculated value of 1.206 g/cm^3 (experimental 1.284 g/cm^3).[17] Improvements to the [Chol]-based ionic liquid parameters are difficult, owing to the lack of experimental data available for refinement.

Densities were also computed for 11 ionic liquid combinations over temperatures ranging from 5 to 90 °C and compared with experimentally observed values (Table 9). Various chain lengths were tested for [RMIM] from R = Et to Oct with multiple anions, [BF_4], [PF_6], [$AlCl_4$], and [TfO]. The relative deviations from experiment were ca. 1−3% with the exception of [EMIM][$AlCl_4$], which gave deviations of ca. 4−5%, similar to the simulations at 25 °C. The general trend of a decreasing density as temperature increases was reproduced for all ionic liquids tested (Figure 7). Good agreement was also found between the fully transferable parameters and the charge/torsion set specific to [EMIM] and [BMIM] (Table 9).

Heats of Vaporization. Ionic liquids are generally characterized by vaporization enthalpies that are almost 1 order of magnitude higher than for molecular liquids because of strong electrostatic interactions between the ions.[1] The importance of properly reproducing the heats of vaporization, ΔH_{vap}, in addition to densities for ionic liquids cannot be minimized, as they both serve as key properties representative of molecular size and the average intermolecular interactions.[30] Heats of vaporization are readily computed from the simulation results using equation 5.

$$\Delta H_{vap} = \Delta H_{gas} - \Delta H_{liquid} = E_{total}(gas) - E_{total}(liquid) + RT \quad (5)$$

Experimental evidence suggests that ionic liquids go into the vapor phase in ion pairs.[36] Hence, the E_{total}(gas) term was computed from the average intra- and intermolecular energy for the ion pair in the gas phase from each ionic liquid combination. E_{total}(liquid) is the total potential energy of the liquid consisting of both the average intramolecular energy, E_{intra}(liquid), and the average intermolecular energy, E_{inter}(liquid), from the ionic liquid. The *RT* term is used in place of a *PV*-work term in the enthalpy. The heats of vaporization

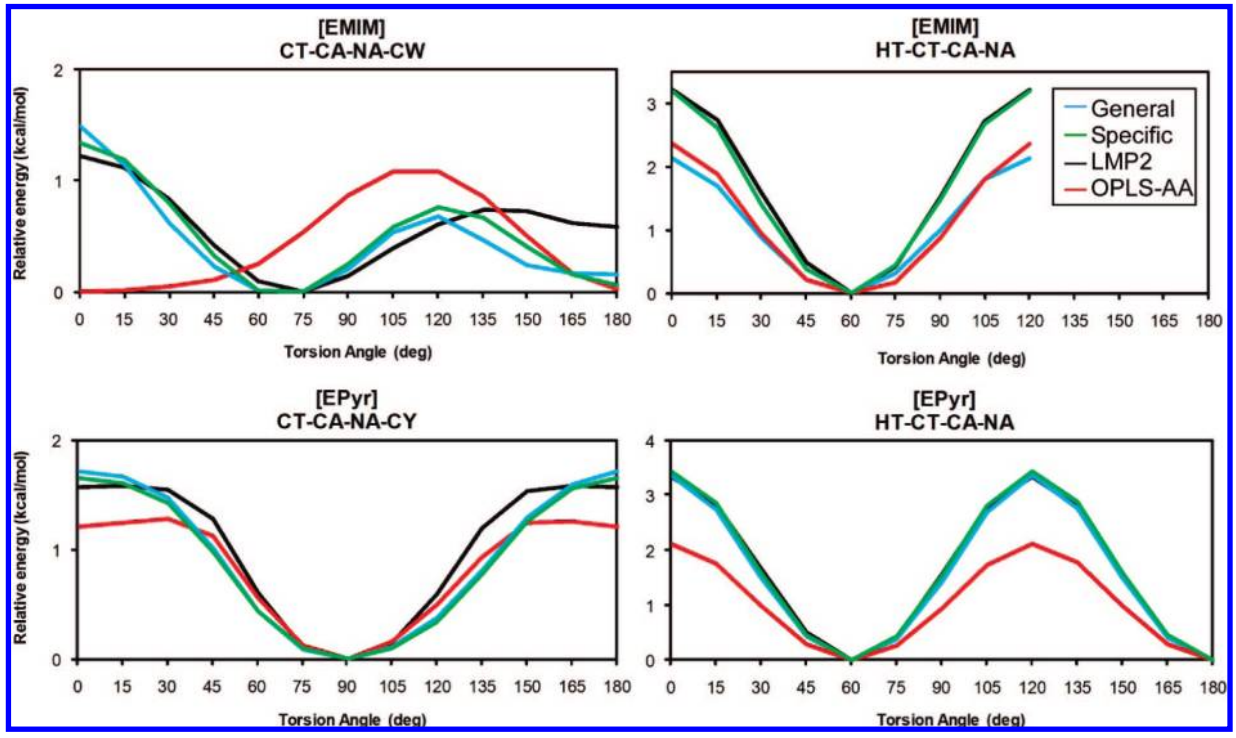

Figure 5. Torsion energy profiles for the rotation around dihedral angles for [EMIM] and [EPyr] cations. The transferable [RMIM] and [RPyr] parameters given in blue, parameters specific to [EMIM] and [EPyr] in green, LMP2/cc-pVTZ(-f)/HF/6−31G(d) in black, and the unaltered OPLS-AA force field in red.

obtained from the MC simulations for the ionic liquids are presented in Tables 6−8, and for [RMIM] in Figure 8.

Comparison between the computed and experimental heats of vaporization, ΔH_{vap}, values is particularly difficult, owing to the large reported deviations between different experimental-based techniques. For example, earlier ΔH_{vap} estimates derived from correlations of Hildebrand's solubility parameter, δ, to solvent-controlled chemical reactions[50] and viscosity data[73] have been found to significantly overestimate experimentally measured ΔH_{vap} values.[1] Accordingly, the new ionic liquid parameters were not adjusted to improve agreement with reported experimental data. Instead, the parameters were fit to reproduce ab initio calculations and directly compared to available experimental values. The MC simulations gave favorable correlations with direct measurements of the ionic liquids using a temperature programmed desorption technique[36] and with more accurate ΔH_{vap} estimates derived from density and surface tensions measurements coupled to Zaitsau et. al's empirical equation.[60] For example, ΔH_{vap} values of 41.9 and 38.3 kcal/mol were computed for the chloroaluminate ionic liquids [BMIM]-[$AlCl_4$] and [HMIM][$AlCl_4$], respectively, using the general [RMIM] parameter set which were found to be in close agreement with the experimentally estimated values of 41.1 and 39.5 kcal/mol.[60] Calculations of [OMIM]-based ionic liquids with [BF_4] and [PF_6] counteranions gave ΔH_{vap} values of 41.9 and 47.3 kcal/mol, respectively, in reasonable agreement with experimentally measured values of 38.7 ± 0.7 and 40.4 ± 1.0 kcal/mol.[36] The computed ΔH_{vap} values of 27.8 and 31.9 kcal/mol for [BMIM][BF_4] and [BMIM][PF_6], respectively, are in good agreement with recent experimental estimates of 30.6 and 37.0 kcal/mol;[49] the simulations confirm earlier estimates of 48.6 and 45.8 kcal/mol[50] from correlations of Hildebrand's solubility parameter to be overestimated.[1] Further comparisons of calculated versus experimental ΔH_{vap} values for [RMIM]-based ionic liquids are given in Table 6.

A general trend found in the calculation of the ΔH_{vap} was a smaller predicted value in the [EMIM] cation-based ionic liquids relative to other [RMIM] values. For example, [RMIM][NO_3] ΔH_{vap} values of 31.8, 18.1, and 28.0 kcal/mol were computed using the general OPLS-AA parameter set for [MMIM], [EMIM], and [BMIM], respectively. Experimental combustion calorimetry in conjunction with ab initio calculations (G3MP2) estimate ΔH_{vap} as 39.1 ± 1.3 and 38.8 ± 1.4 kcal/mol for [EMIM] and [BMIM] in the [NO_3]-based ionic liquids.[62] The computed heats of vaporization are particularly sensitive to the charge sets used, as the specific OPLS-AA charge set reduced the deviation between the ionic liquids and brought the results closer to the estimates with computed values of 25.8 and 31.9 kcal/mol for [EMIM][NO_3] and [BMIM][NO_3]. The general parameters maybe more susceptible to deviations for [EMIM] because of the use of the same atom types CT and HT to model the end carbon and hydrogens as the longer alkyl side chains, such as butyl and hexyl. Earlier parametrization efforts used an atom type specific to [EMIM] to cap the alkyl chain.[23] The use of a polarizable force field may also improve agreement.[74] However, the large differences in the computed ΔH_{vap} values when using the transferable and cation specific OPLS-AA parameters were not seen for the predicted densities (Figure 6) which were generally insensitive to the charge/torsion set used.

Table 6. Calculated and Experimental Liquid Densities (g/cm^3) and Heats of Vaporization (kcal/mol) at 25 °C for 1-Alkyl-3-methylimidazolium [RMIM]-Based Ionic Liquids[a]

ionic liquid	density (calcd)	density (exptl)	refs	ΔH_{vap} (calcd)	ΔH_{vap} (exptl)	refs
[MMIM][BF_4]	1.299	1.373	44	30.1		
[EMIM][BF_4]	1.254 (1.253)	1.279, 1.28	45, 46	18.0 (24.0)		
[BMIM][BF_4]	1.171 (1.178)	1.19, 1.21, 1.26	45, 47, 48	27.8 (30.0)	*30.6*,[e] *48.6*[f]	49, 50
[HMIM][BF_4]	1.105	1.1481, 1.1484, 1.177	44, 51	35.8		
[OMIM][BF_4]	1.044	1.08, 1.0912, 1.105, 1.133	44, 48, 52, 53	41.9	38.7 ± 0.7,[g] *29.2*[e]	36, 49
[MMIM][PF_6]	1.512			33.1		
[EMIM][PF_6]	1.455 (1.455)	1.558[b]	54	21.4 (27.6)		
[BMIM][PF_6]	1.339 (1.342)	1.31, 1.36, 1.368, 1.37	44, 48, 55, 56	31.9 (31.9)	*37.0*,[e] *45.8*[f]	49, 50
[HMIM][PF_6]	1.257	1.24, 1.278, 1.29, 1.292, 1.2935	47, 51, 55, 56	40.1	*33.4*[e]	49
[OMIM][PF_6]	1.181	1.19, 1.22, 1.237	48, 55, 56	47.3	40.4 ± 1.0,[g] *34.5*[e]	36, 49
[MMIM][Cl]	1.175	1.155	57	32.3		
[EMIM][Cl]	1.121 (1.130)	1.110	57	19.3 (25.5)		
[BMIM][Cl]	1.041 (1.060)	1.075, 1.08	55, 57	29.1 (32.0)		
[HMIM][Cl]	1.007	1.03, 1.0338	55, 58	37.5		
[OMIM][Cl]	0.959	1.00, 1.0104, 1.0124	55, 58, 59	44.6	*29.3*[e]	49
[MMIM][$AlCl_4$]	1.260	1.3289	60	31.1	*45.3*[e]	60
[EMIM][$AlCl_4$]	1.226 (1.229)	1.2947, 1.302	24, 60	19.8 (26.3)	*43.6*[e]	60
[BMIM][$AlCl_4$]	1.175 (1.176)	1.238, 1.2381	24, 60	41.9 (32.1)	*41.1*[e]	60
[HMIM][$AlCl_4$]	1.120	1.1952	60	38.3	*39.5*[e]	60
[MMIM][Al_2Cl_7]	1.282	1.341[c]	57, 61	34.0		
[EMIM][Al_2Cl_7]	1.260 (1.249)	1.325[c]	57, 61	22.3 (28.2)		
[BMIM][Al_2Cl_7]	1.206 (1.203)	1.272[c]	57, 61	32.4 (33.6)		
[HMIM][Al_2Cl_7]	1.119			39.2		
[MMIM][NO_3]	1.305			31.8		
[EMIM][NO_3]	1.253 (1.258)			18.1 (25.8)	*39.1 ± 1.3*[h]	62
[BMIM][NO_3]	1.163 (1.175)	1.15343	58	28.0 (31.9)	*38.8 ± 1.4*[h]	62
[HMIM][NO_3]	1.080	1.11658	58	34.9		
[MMIM][TfO]	1.489			32.5		
[EMIM][TfO]	1.420 (1.412)	1.37522, 1.38, 1.390	47, 63 64	21.3 (26.7)		
[BMIM][TfO]	1.297 (1.310)	1.30, 1.30148, 1.3013[d]	64, 65	31.1 (32.7)	*33.8*[f]	50
[HMIM][TfO]	1.241	1.24	64	40.6		
[OMIM][TfO]	1.125	1.12	64, 66	46.5	36.1 ± 0.7[g]	36

[a] Calculated density and ΔH_{vap} values given in parentheses were computed using OPLS-AA charge/torsion parameters specific to [EMIM] and [BMIM]. ΔH_{vap} estimations from experimental data given in italics. R = M (methyl), E (ethyl), B (butyl), H (hexyl), and O (octyl). [b] 23 °C; density computed from crystal structure cell parameters. [c] [RMIM][Cl]−$AlCl_3$ 0.66 melt,[57] which should correspond to exclusively [RMIM][Al_2Cl_7].[61] [d] 22.6 °C. [e] Experimental density and surface tension measurements in conjunction with Kabo's equation[49] was used to estimate ΔH_{vap}. [f] ΔH_{vap} estimated from Hildebrand's solubility parameter, δ, to solvent-controlled Diels−Alder reaction. [g] Temperature-programmed desorption. [h] Experimental combustion calorimetry in conjunction with ab initio calculations (G3MP2) were used to estimate ΔH_{vap}.

Table 7. Calculated Liquid Densities (g/cm^3) and Heats of Vaporization (kcal/mol) at 25 °C for *N*-Alkylpyridinium [RPyr] (R = Me, Et, Bu, Hex, Oct)-Based Ionic Liquids[a]

ionic liquid	density	ΔH_{vap}	ionic liquid	density	ΔH_{vap}
[MPyr][BF_4]	1.300 (1.302)	41.5 (41.0)	[MPyr][PF_6]	1.514 (1.520)	44.9 (44.3)
[EPyr][BF_4][b]	1.250 (1.256)	37.3 (29.8)	[EPyr][PF_6]	1.462 (1.459)	40.3 (33.5)
[BPyr][BF_4][c]	1.169 (1.176)	28.7 (41.1)	[BPyr][PF_6]	1.345 (1.347)	29.8 (39.0)
[HPyr][BF_4][d]	1.091	43.8	[HPyr][PF_6]	1.247	46.2
[OPyr][BF_4]	1.043	52.2	[OPyr][PF_6]	1.170	53.8
[MPyr][$AlCl_4$]	1.246 (1.253)	41.5 (41.3)	[MPyr][Al_2Cl_7]	1.271 (1.267)	44.1 (40.7)
[EPyr][$AlCl_4$]	1.221 (1.217)	37.8 (30.6)	[EPyr][Al_2Cl_7]	1.261 (1.241)	40.8 (28.9)
[BPyr][$AlCl_4$]	1.163 (1.161)	28.1 (36.3)	[BPyr][Al_2Cl_7]	1.181 (1.194)	29.7 (38.9)
[MPyr][NO_3]	1.312 (1.315)	41.6 (41.5)	[MPyr][TfO]	1.506 (1.504)	43.7 (42.5)
[EPyr][NO_3]	1.253 (1.263)	36.4 (29.5)	[EPyr][TfO]	1.421 (1.431)	38.4 (31.6)
[BPyr][NO_3]	1.161 (1.167)	25.2 (35.3)	[BPyr][TfO]	1.306 (1.318)	27.1 (37.3)
[MPyr][Cl]	1.181 (1.184)	44.9 (43.8)	[HPyr][Cl]	1.006	46.5
[EPyr][Cl]	1.122 (1.130)	39.3 (31.9)	[OPyr][Cl]	0.943	52.8
[BPyr][Cl]	1.041 (1.050)	28.3 (38.8)			

[a] Calculated density and ΔH_{vap} values given in parentheses were computed using OPLS-AA charge/torsion parameters specific to [MPyr], [EPyr], and [BPyr]. [b] Experimental density of 1.3020 g/cm^3.[67] [c] Experimental density of 1.2144 and 1.22 g/cm^3.[46,53] [d] Experimental density of 1.16 g/cm^3 at 20 °C.[68]

Kemp Elimination. As an initial test of the newly developed ionic liquid parameters, mixed quantum and molecular mechanical (QM/MM) calculations were carried out on the Kemp elimination of benzisoxazole with piperidine in [BMIM][PF_6] (Scheme 1). The solutes were treated with the PDDG/PM3 semiempirical QM method.[75] PDDG/PM3 has given excellent results in our recent QM/MM studies of the Kemp elimination of 5-nitro-benzisoxazole via catalytic antibody 4B2[76] and the condensed-phase Kemp decarboxylation of benzisoxazole-3-carboxylic acid.[77] Potentials of

Table 8. Calculated Liquid Densities (g/cm^3) and Heats of Vaporization (kcal/mol) at 25 °C for Choline [Chol]-Based Ionic Liquids

ionic liquid	density	ΔH_{vap}	ionic liquid	density	ΔH_{vap}
[Chol][Cl][a]	1.040	78.9	[Chol][$AlCl_4$]	1.192	75.3
[Chol][Ace][b]	1.206	70.9	[Chol][Al_2Cl_7]	1.195	77.5
[Chol][Sacc][c]	1.200	79.2	[Chol][NO_3]	1.159	76.9
[Chol][BF_4]	1.165	75.7	[Chol][TfO]	1.326	76.0
[Chol][PF_6]	1.375	77.8			

[a] Experimental density from crystal structure at 85 °C is 1.12 g/cm^3.[69] [b] Experimental density is 1.284 g/cm^3.[17] [c] Experimental density is 1.383 g/cm^3.[17]

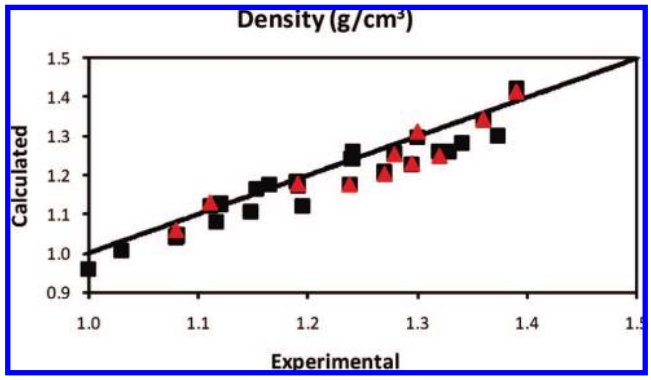

Figure 6. Computed OPLS-AA and experimental results for liquid densities for 1-alkyl-3-methylimidazolium [RMIM]-based ionic liquids (black squares) at 25 °C and 1 atm. Computed values with OPLS-AA parameters specific to [EMIM] and [BMIM] given as red triangles.

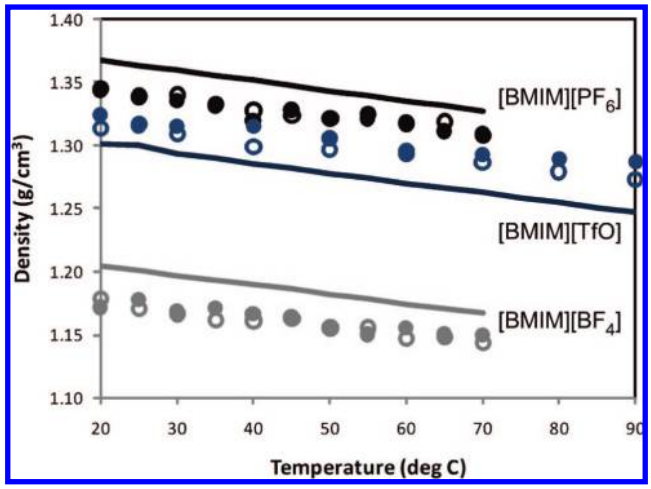

Figure 7. Calculated and experimental liquid densities versus temperature for 1-butyl-3-methylimidazolium [BMIM]-based ionic liquids with [BF_4] in black, [TfO] in blue, and [PF_6] in gray. (○ = general OPLS-AA [RMIM] parameter set, ● = specific OPLS-AA [BMIM] parameter set, and solid lines = experimental values).

mean force (PMF) calculations coupled to Metropolis Monte Carlo (MC) statistical mechanics were used to build a free-energy profile for the ring opening at 25 °C and 1 atm.

A reacting distance, $R_{NH} - R_{CH}$, was used for the proton transfer between the nitrogen on piperidine and the hydrogen on the isoxazole ring (Figure 9); $R_{NH} + R_{CH}$ was kept constant at 2.85 Å. The fixed distance of 2.85 Å was determined to be appropriate from our recent study of the reaction.[76] A second perturbation was necessary, R_{NO}, which entailed the opening of the isoxazole ring via an increasing N−O distance. Combining the $R_{NH} - R_{CH}$ PMF which runs along one reaction coordinate with the R_{NO} PMF in a second direction produced a two-dimensional (2D) PMF. The result is a free-energy map that can be used to identify minima and the transition state present in the reaction. The breaking of the N−O bond was split into ca. 24 windows with an increment of 0.04 Å. Each PMF calculation required 5 million configurations of equilibration followed by 10 million configurations of averaging.

For the hydrogen transfer, a novel method was developed in our recent study of the ring-opening of 5-nitrobenzisoxazole, where it was found that free-energy changes for individual windows can be fit almost perfectly by a fifth order polynomial.[76] Using only 7 windows out of the usual 50 and analytically integrating the values yielded a sextic polynomial for the overall proton-transfer PMF that is essentially identical to running the full simulation. The new methodology provided a 7-fold improvement in speed over traditional PMF methods for the enzymatic calculations, and the largest deviation found between the approximate and the detailed calculation was 1 kcal/mol. The fifth order polynomial quadrature method was used to compute the free energy of activation for the Kemp elimination in a periodic box of 378 [BMIM][PF_6] ionic liquid ions in the NPT ensemble. Ewald sums were used to handle the long-range electrostatics, and electrostatic contributions to the solute−solvent energy were calculated using CM3 charges,[78] with a scale factor of 1.14.

The free-energy surface for the Kemp elimination of benzisoxazole via piperidine is shown in Figure 10. The reaction follows a concerted mechanism where the R_{NO} distance of the isoxazole ring in the transition structure is 2.06 Å while the R_{NH} and R_{CH} distances are 1.10 and 1.75 Å, respectively. Computed changes in free energy yielded a $\Delta G^{\ddagger}$ value of 25.2 kcal/mol after a cratic entropy correction of 1.89 kcal/mol.[79] The level of uncertainty is less than ±1 kcal/mol based on fluctuations in the averages for the individual free-energy perturbation (FEP) windows. The experimental $\Delta G^{\ddagger}$ for the reaction under the same conditions is 22.6 ± 0.5 kcal/mol.[80] The calculations reproduce the activation values well, particularly when considering the computed and experimental uncertainties and the additional overestimation of ca. 1 kcal/mol for the Kemp elimination from the fifth order polynomial methodology.[76] The good agreement suggests that the ionic liquid microenvironment is being appropriately modeled by the new parameters. Further calculations and a detailed analysis of the Kemp elimination in additional ionic liquids and conventional solvents with different bases are currently underway and will be the focus of a future publication.

Conclusions

The development and testing of the OPLS-AA force field for use in the simulation of 68 unique ionic liquids has been described. Charges, equilibrium geometries, and torsional Fourier coefficients were derived to reproduce gas-phase structures and conformational energetics from LMP2/cc-

Table 9. Calculated and Experimental Liquid Densities (g/cm^3) versus Temperature for 1-Alkyl-3-methylimidazolium [RMIM] and *N*-Alkylpyridinium [RPyr] (R = Me, Et, Bu, Hex, Oct)-Based Ionic Liquids[a]

ionic liquid	temp (°C)	density (calcd)	density (exptl)	refs	ionic liquid	temp (°C)	density (calcd)	density (exptl)	refs
[EMIM][BF_4]	20	1.255 (1.260)	1.283	46	[BMIM][TfO]	20	1.314 (1.324)	1.3013	70
	25	1.253 (1.254)	1.279	46		25	1.317 (1.315)	1.30, 1.30148	64, 65
	30	1.255 (1.251)	1.275	46		30	1.309 (1.315)	1.2934	70
	35	1.246 (1.251)	1.271	46		40	1.299 (1.315)	1.2856	70
	40	1.247 (1.246)	1.266	46		50	1.296 (1.305)	1.277	70
[EMIM][TfO]	5	1.431 (1.428)	1.40052	63		60	1.293 (1.296)	1.2699	70
	15	1.431 (1.420)	1.39204	63		70	1.286 (1.293)	1.2623	70
	25	1.425 (1.422)	1.38360	63		80	1.279 (1.289)	1.2545	70
	35	1.414 (1.411)	1.37522	63		90	1.273 (1.288)	1.2469	70
	45	1.412 (1.414)	1.36690	63	[HMIM][BF_4]	25	1.102	1.14532	71
	55	1.401 (1.404)	1.35863	63		35	1.094	1.13851	71
	65	1.397 (1.391)	1.35043	63		45	1.097	1.13167	71
	75	1.393 (1.385)	1.34230	63		55	1.088	1.12489	71
[EMIM][$AlCl_4$]	10	1.240 (1.244)	1.3060	60		65	1.080	1.11816	71
	15	1.238 (1.239)	1.3020	60		75	1.077	1.11147	71
	20	1.234 (1.228)	1.2979	60		85	1.070	1.10484	71
	25	1.229 (1.229)	1.2947	60	[HMIM][PF_6]	5	1.267	1.3101	72
	30	1.222 (1.224)	1.2908	60		10	1.265	1.3060	72
	35	1.221 (1.216)	1.2870	60		15	1.266	1.3019	72
	40	1.217 (1.216)	1.2833	60		20	1.262	1.2979	72
	45	1.214 (1.214)	1.2798	60		25	1.255	1.2937, 1.29341	71, 72
	50	1.209 (1.206)	1.2759	60		30	1.253	1.2896	72
	55	1.207 (1.200)	1.2725	60		35	1.256	1.2854, 1.28578	71, 72
	60	1.203 (1.201)	1.2689	60		40	1.249	1.2813	72
	65	1.200 (1.195)	1.2651	60		45	1.250	1.2772, 1.27792	71, 72
[BMIM][BF_4]	20	1.179 (1.172)	1.2049, 1.2038	70		55	1.244	1.26988	71
	25	1.171 (1.178)	1.2011, 1.2000	70		65	1.237	1.26213	71
	30	1.167 (1.169)	1.1974, 1.1962	70		75	1.232	1.25436	71
	35	1.161 (1.171)	1.1938, 1.1924	70		85	1.229	1.24681	71
	40	1.161 (1.167)	1.1901, 1.1889	70	[OMIM][BF_4]	25	1.034	1.0912	53
	45	1.168 (1.165)	1.1865, 1.1854	70		30	1.037	1.0887	53
	50	1.155 (1.155)	1.1827, 1.1813	70		40	1.039	1.0823	53
	55	1.167 (1.174)	1.1790, 1.1779	70		50	1.028	1.0747	53
	60	1.147 (1.155)	1.1753, 1.1741	70		60	1.027	1.0685	53
	65	1.162 (1.151)	1.1717, 1.1705	70		70	1.025	1.0618	53
	70	1.143 (1.150)	1.1680, 1.1669	70	[OMIM][PF_6]	25	1.178	1.2245	53
[BMIM][PF_6]	20	1.345 (1.343)	1.3698, 1.3681	70		30	1.163	1.2207	53
	25	1.339 (1.338)	1.3657, 1.3641	70		40	1.161	1.2141	53
	30	1.340 (1.335)	1.3616, 1.3600	70		50	1.159	1.2069	53
	35	1.333 (1.331)	1.3574, 1.3557	70		60	1.156	1.1999	53
	40	1.328 (1.319)	1.3533, 1.3518	70		70	1.149	1.1922	53
	45	1.324 (1.328)	1.3492, 1.3475	70	[BPyr][BF_4]	25	1.175 (1.177)	1.2144	53
	50	1.322 (1.321)	1.3451, 1.3435	70		30	1.175 (1.177)	1.2118	53
	55	1.325 (1.321)	1.3410, 1.3394	70		40	1.165 (1.172)	1.2053	53
	60	1.318 (1.318)	1.3369, 1.3352	70		50	1.162 (1.164)	1.1988	53
	65	1.319 (1.311)	1.3327, 1.3311	70		60	1.155 (1.163)	1.1922	53
	70	1.308 (1.309)	1.3286, 1.3270	70		70	1.148 (1.156)	1.1856	53

[a] Calculated density values given in parentheses were computed using OPLS-AA charge/torsion parameters specific to [EMIM], [BMIM], [HMIM], [OMIM], and [BPyr], respectively.

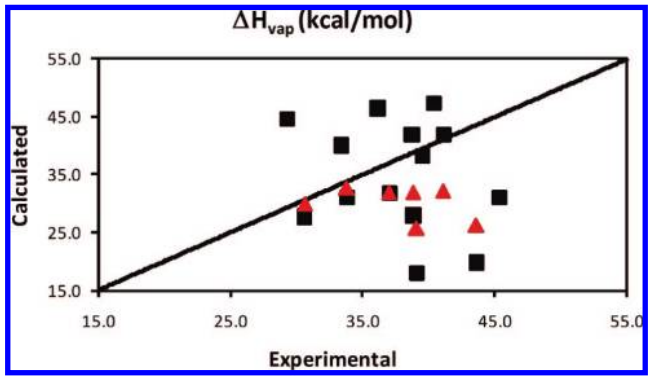

Figure 8. Computed OPLS-AA and experimental results for heats of vaporization for 1-alkyl-3-methylimidazolium [RMIM]-based ionic liquids (black squares) at 25 °C and 1 atm. Computed values with OPLS-AA parameters specific to [EMIM] and [BMIM] given as red triangles.

pVDZ(-f)//HF/6−31G(d) quantum mechanical calculations. Multiple alkyl chain lengths were considered in the fitting process, and the quality of the fits for the transferable force field yielded energy profiles for bond rotations comparable to that of ab initio calculations. In addition, the highly transferable parameters for [RMIM] and [RPyr] were compared to potentials developed specifically for individual ionic liquid cations and good agreement in liquid densities values was found between both sets. Relative deviations from experimental density values were ca. 1−3%; however, chloroaluminate-based ionic liquids had slightly larger deviations at ca. 4−5%. The errors in the densities computed for choline-based ionic liquids were significantly larger but are difficult to improve, owing to the lack of available experimental data for refinement. Agreement between the computed

Scheme 1. Kemp Elimination Reaction of Benzisoxazole with Piperidine

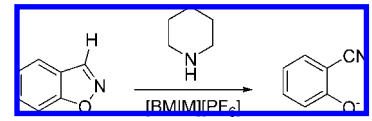

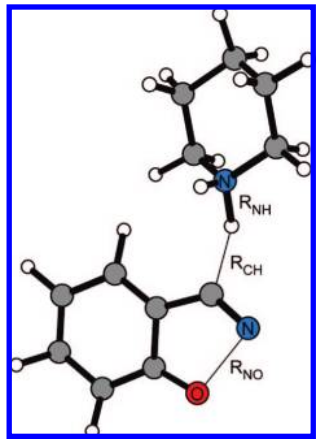

Figure 9. Reaction coordinates, $R_{NH} - R_{CH}$ and R_{NO}, used to locate stationary points from free-energy maps obtained via PMF simulations for the Kemp elimination of benzisoxazole using piperidine. Illustrated structure corresponds to the transition state computed from QM/MM calculations.

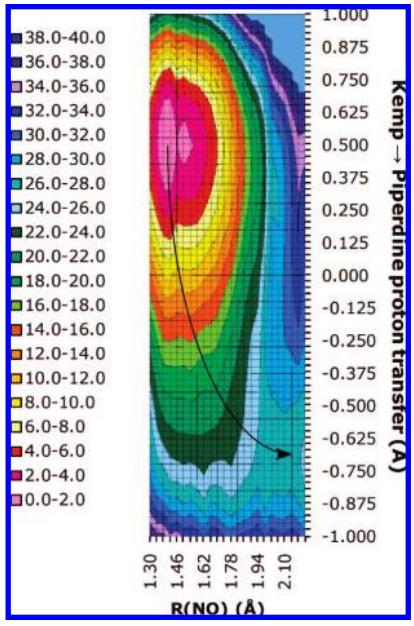

Figure 10. Two-dimensional potentials of mean force (free energy map, kcal/mol) for the Kemp elimination reaction of benzisoxazole via piperidine in [BMIM][PF_6]. Free energy values truncated to 40 kcal/mol for clarity. The arrow follows the reaction path toward product.

ΔH_{vap} and experimental estimates are generally good; however, absolute errors in the vaporization enthalpies are more difficult to assess because of inconsistencies between reported experimental values. In addition, the computed heats of vaporization were found to be more sensitive to the charge set used. The importance of testing the cation and anion parameters in a large number of ionic liquid combinations is highlighted in this work by the liquid simulation of an unprecedented number of ionic liquids, with 35 of the 68 solvents recomputed using specific cation parameters for a detailed comparison of the new parameters set's transferability between different alkyl chain lengths and anion combinations. QM/MM simulations for the Kemp elimination of benzisoxazole using piperidine as the base in [BMIM][PF_6] yielded good agreement with the experimental free energy of activation, i.e., $\Delta G^{\ddagger}$(calcd) = 25.2 ± 1 kcal/mol compared to $\Delta G^{\ddagger}$(exptl) = 22.6 ± 0.5 kcal/mol.[80]

Acknowledgment. Gratitude is expressed to the Alabama Supercomputer Center and Auburn University for support of this research and to Dr. Kasper P. Jensen for helpful discussions.

Supporting Information Available: ESP charges specific to [EMIM], [MPyr], and [EPyr]. Equilibrium bond and angle reference values, r_o and θ_o, and force constants, k, for the simulations. Additional torsion Fourier coefficients for the cations. Additional torsion energy profiles for the cations. Box sizes for all ionic liquids simulated. This material is available free of charge via the Internet at http://pubs.acs.org.

References

(1) Weingaertner, H. *Angew. Chem., Int. Ed.* **2008**, *47*, 654–670.

(2) (a) Forsyth, S. A.; Pringle, J. M.; MacFarlane, D. R. *Aust. J. Chem.* **2004**, *57*, 113–119. (b) Welton, T. *Chem. Rev.* **1999**, *99*, 2071–2083. (c) Seddon, K. R. *J. Chem. Tech. Biotechnol.* **1997**, *68*, 351–356.

(3) Bonhote, P.; Dias, A.-P.; Papageorgiou, N.; Kalyanasundaram, K.; Gratzel, M. *Inorg. Chem.* **1996**, *35*, 1168–1178.

(4) (a) Iwata, K.; Okajima, H.; Saha, S.; Hamaguchi, H. *Acc. Chem. Res.* **2007**, *40*, 1174–1181. (b) Castner, E. W.; Wishart, J. F.; Shirota, H. *Acc. Chem. Res.* **2007**, *40*, 1217–1227.

(5) (a) Hardacre, C.; Holbrey, J. D.; Nieuwenhuyzen, M.; Youngs, T. G. A. *Acc. Chem. Res.* **2007**, *40*, 1146–1155. (b) Hardacre, C.; Holbrey, J. D.; McMath, S. E. J. *J. Chem. Phys.* **2003**, *118*, 273–278.

(6) (a) MacFarlane, D. R.; Forsyth, M.; Howlett, P. C.; Pringle, J. M.; Sun, J.; Annat, G.; Neil, W.; Izgorodina, E. I. *Acc. Chem. Res.* **2007**, *40*, 1165–1173. (b) Tsuda, T.; Hussey, C. L. *Electrochem. Soc. Interface* **2007**, *16*, 42–49. (c) Silvester, D. S.; Compton, R. G. *Z. Phys. Chem.* **2006**, *220*, 1247–1274.

(7) (a) Han, X.; Armstrong, D. W. *Acc. Chem. Res.* **2007**, *40*, 1079–1086. (b) Visser, A. E.; Swatloski, R. P.; Reichert, W. M.; Davis, J. H., Jr.; Rogers, R. D.; Mayton, R.; Sheff, S.; Wierzbicki, A. *Chem. Commun.* **2001**, 135–136. (c) Huddleston, J. G.; Rogers, R. D. *Chem. Commun.* **1998**, 1765–1766.

(8) Pârvulescu, V. I.; Hardacre, C. *Chem. Rev.* **2007**, *107*, 2615–2665.

(9) van Rantwijk, F.; Sheldon, R. A. *Chem. Rev.* **2007**, *107*, 2757–2785.

(10) (a) Welton, T. *Coord. Chem. Rev.* **2004**, *248*, 2459–2477. (b) Wasserscheid, P.; Keim, W. *Angew. Chem., Int. Ed.* **2000**, *39*, 3772–3789.

(11) (a) Sheldon, R. *Chem. Commun.* **2001**, 2399–2407. (b) Haumann, M.; Riisager, A. *Chem. Rev.* **2008**, *108*, 1474–1497. (c) Zhang, Z. C. *Adv. Catal.* **2006**, *49*, 153–237.

(12) (a) Smiglak, M.; Metlen, A.; Rogers, R. D. *Acc. Chem. Res.* **2007**, *40*, 1182–1192. (b) Lodge, T. P. *Science* **2008**, *321*, 50–51.

(13) Binnemans, K. *Chem. Rev.* **2007**, *107*, 2592–2614.

(14) (a) Ranke, J.; Stolte, S.; Störmann, R.; Arning, J.; Jastorff, B. *Chem. Rev.* **2007**, *107*, 2183–2206. (b) Docherty, K. M.; Kulpa, C. F., Jr. *Green Chem.* **2005**, *7*, 185–189. (c) Stolte, S.; Arning, J.; Bottin-Weber, U.; Matzke, M.; Stock, F.; Thiele, K.; Uerdingen, M.; Welz-Biermann, U.; Jastorff, B.; Ranke, J. *Green Chem.* **2006**, *8*, 621–629.

(15) Wells, A. S.; Coombe, V. T. *Org. Process Res. Dev.* **2006**, *10*, 794–798.

(16) Gathergood, N.; Garcia, M. T.; Scammels, P. J. *Green Chem.* **2004**, *6*, 166–175.

(17) Nockemann, P.; Thijs, B.; Driesen, K.; Janssen, C. R.; Van Hecke, K.; Van Meervelt, L.; Kossmann, S.; Kirchner, B.; Binnemans, K. *J. Phys. Chem. B* **2007**, *111*, 5254–5263.

(18) Gathergood, N.; Scammels, P. J.; Garcia, M. T. *Green Chem.* **2006**, *8*, 156–160.

(19) Fukumotu, K.; Yoshizawa, M.; Ohno, H. *J. Am. Chem. Soc.* **2005**, *127*, 2398–2399.

(20) Pernak, J.; Stefaniak, F.; Wglewski, J. *Eur. J. Org. Chem.* **2005**, 650–652.

(21) (a) Lynden-Bell, R. M.; Del Pópolo, M. G.; Youngs, T. G. A.; Kohanoff, J.; Hanke, C. G.; Harper, J. B.; Pinilla, C. C. *Acc. Chem. Res.* **2007**, *2007*, 1138–1145. (b) Pádua, A. A. H.; Costa Gomes, M. F.; Canongia Lopes, J. N. A. *Acc. Chem. Res.* **2007**, *40*, 1087–1096. (c) Wang, Y.; Jiang, W.; Yan, T.; Voth, G. A. *Acc. Chem. Res.* **2007**, *40*, 1193–1199. (d) Cadena, C.; Zhao, Q.; Snurr, R. Q.; Maginn, E. J. *J. Phys. Chem. B* **2006**, *110*, 2821–2832. (e) Hunt, P. A. *Mol. Simul.* **2006**, *31*, 1–10. (f) Canongia Lopes, J. N.; Padua, A. H. *J. Phys. Chem. B* **2004**, *108*, 16893–16898. (g) Liu, Z.; Huang, S.; Wang, W. *J. Phys. Chem. B* **2004**, *108*, 12978–12989. (h) Morrow, T. I.; Maginn, E. J. *Fluid Phase Equilib.* **2004**, *217*, 97–104. (i) de Andrade, J.; Böes, E. S.; Stassen, H. *J. Phys. Chem. B* **2002**, *106*, 3546–3548.

(22) Canongia Lopes, J. N.; Padua, A. A. H. *J. Phys. Chem. B* **2006**, *110*, 19586–19592.

(23) Canongia Lopes, J. N.; Deschamps, J.; Padua, A. H. *J. Phys. Chem. B* **2004**, *108*, 2038–2047.

(24) de Andrade, J.; Böes, E. S.; Stassen, H. *J. Phys. Chem. B* **2002**, *106*, 13344–13351.

(25) Acevedo, O.; Jorgensen, W. L.; Evanseck, J. D. *J. Chem. Theory Comput.* **2007**, *3*, 132–138.

(26) MacKerell, A. D., Jr.; Bashford, D.; Bellott, M.; Dunbrack, R. L.; Evanseck, J. D.; Field, M. J.; Fisher, S.; Gao, J.; Guo, H.; Ha, S.; Joseph-McCarthy, S.; Kuchnir, L.; Kuczera, K.; Lau, F. T. K.; Mattos, C.; Michnick, S.; Ngo, T.; Nguyen, D. T.; Prodhom, B.; Reiher, W. E., III; Roux, B.; Schlenkrich, M.; Smith, J. C.; Stote, R.; Straub, J.; Watanabe, M.; Wiorkiewicz-Kuczera, J.; Yin, D.; Karplus, M. *J. Phys. Chem. B* **1998**, *102*, 3586.

(27) Cornell, W. D.; Cieplak, P.; Bayly, C. I.; Gould, I. R.; Merz, K. M.; Ferguson, D. M.; Spellmeyer, D. C.; Fox, T.; Caldwell, J. W.; Kollman, P. A. *J. Am. Chem. Soc.* **1995**, *117*, 5179–5197.

(28) Jorgensen, W. L.; Maxwell, D. S.; Tirado-Rives, J. *J. Am. Chem. Soc.* **1996**, *118*, 11225–11236.

(29) (a) Jensen, K. P.; Jorgensen, W. L. *J. Chem. Theory Comput.* **2006**, *2*, 1499–1509. (b) Price, M. L. P.; Ostrovsky, D.; Jorgensen, W. L. *J. Comput. Chem.* **2001**, *22*, 1340–1352. (c) Rizzo, R. C.; Jorgensen, W. L. *J. Am. Chem. Soc.* **1999**, *121*, 4827–4836. (d) Jorgensen, W. L.; McDonald, N. A. *J. Phys. Chem. B* **1998**, *102*, 8049–8059.

(30) Jorgensen, W. L.; Tirado-Rives, J. *Proc. Nat. Acad. Sci. U.S.A.* **2005**, *102*, 6665–6670.

(31) (a) Kaminski, G. A.; Friesner, R. A.; Tirado-Rives, J.; Jorgensen, W. L. *J. Phys. Chem. B* **2001**, *105*, 6474–6487. (b) Watkins, E. K.; Jorgensen, W. L. *J. Phys. Chem. A* **2001**, *105*, 4118–4125.

(32) Jaguar, version 6.0, Schrödinger, LLC, New York, NY, 2005.

(33) (a) Saebø, S.; Pulay, P. *Annu. Rev. Phys. Chem.* **1993**, *44*, 213–236. (b) Saebø, S.; Tong, W.; Pulay, P. *J. Chem. Phys.* **1993**, *98*, 2170–2175.

(34) Dunning, T. H., Jr. *J. Chem. Phys.* **1989**, *90*, 1007–1023.

(35) Jorgensen, W. L.; Tirado-Rives, J. *J. Comput. Chem.* **2005**, *26*, 1689–1700.

(36) Armstrong, J. P.; Hurst, C.; Jones, R. G.; Licence, P.; Lovelock, K. R. J.; Satterley, C. J.; Villar-Garcia, I. J. *Phys. Chem. Chem. Phys.* **2007**, *9*, 982–990.

(37) McDonald, N. A.; Jorgensen, W. L. *J. Phys. Chem. B* **1998**, *102*, 8049–8059.

(38) Jorgensen, W. L.; McDonald, N. A. *J. Mol. Struct. (THEOCHEM)* **1998**, *424*, 145–155.

(39) Gale, R. J.; Gilbert, B. P.; Osteryoung, R. A. *Inorg. Chem.* **1978**, *17*, 2728–2729.

(40) Wilkes, J. S.; Frye, J. S.; Reynolds, G. F. *Inorg. Chem.* **1983**, *22*, 3870–3872.

(41) (a) Ackermann, B. L.; Tsarbopoulos, A.; Allison, J. *Anal. Chem.* **1985**, *57*, 1766–1768. (b) Wicelinski, S. P.; Gale, R. J.; Pamidimukkala, K. M.; Laine, R. A. *Anal. Chem.* **1988**, *60*, 2228–2232.

(42) Gray, J. L.; Maciel, G. E. *J. Am. Chem. Soc.* **1981**, *103*, 7147–7151.

(43) Franzen, G.; Gilbert, B. P.; Pelzer, G.; Depauw, E. *Org. Mass Spectrom.* **1986**, *21*, 443–444.

(44) Ohlin, C. A.; Dyson, P. J.; Laurenczy, G. *Chem. Commun.* **2004**, 1070–1071.

(45) Nishida, T.; Tashiro, Y.; Yamamoto, M. *J. Fluorine Chem.* **2003**, *120*, 135–141.

(46) Noda, A.; Hayamizu, K.; Watanabe, M. *J. Phys. Chem. B* **2001**, *105*, 4603–4610.

(47) Zhang, S.; Sun, N.; He, X.; Lu, X.; Zhang, X. *J. Phys. Chem. Ref. Data* **2006**, *35*, 1475–1517.

(48) Branco, L. C.; Rosa, J. N.; Ramos, J. J. M.; Afonso, C. A. M. *Chem. Eur. J.* **2002**, *8*, 3671–3677.

(49) Zaitsau, D. H.; Kabo, G. J.; Strechan, A. A.; Paulechka, Y. U.; Tschersich, A.; Verevkin, S. P.; Heintz, A. *J. Phys. Chem. A* **2006**, *110*, 7303–7306.

(50) Swiderski, K.; McLean, A.; Gordon, C. M.; Vaughan, D. H. *Chem. Commun.* **2004**, 2178–2179.

(51) (a) Letcher, T. M.; Reddy, P. *J. Chem. Thermodyn.* **2005**, *37*, 415–421. (b) Letcher, T. M.; Reddy, P. *Fluid Phase Equilib.* **2004**, *219*, 107–112.

(52) Arce, A.; Rodil, E.; Soto, A. *J. Solution Chem.* **2006**, *35*, 63–78.

(53) Gu, Z.; Brennecke, J. F. *J. Chem. Eng. Data* **2002**, *47*, 339–345.

(54) Matsumotoa, K.; Hagiwara, R. *J. Fluorine Chem.* **2007**, *128*, 317–331.

(55) Huddleston, J. G.; Visser, A. E.; Reichert, W. M.; Willauer,

H. D.; Broker, G. A.; Rogers, R. D. *Green Chem.* **2001**, *3*, 156–164.

(56) Dzyuba, S. V.; Bartsch, R. A. *ChemPhysChem* **2002**, *3*, 161–166.

(57) Fannin, A. A., Jr.; Floreani, D. A.; King, L. A.; Landers, J. S.; Piersma, B. J.; Stech, D. J.; Vaughn, R. L.; Wilkes, J. S.; Williams, J. L. *J. Phys. Chem.* **1984**, *88*, 2614–2621.

(58) Seddon, K. R.; Stark, A. S.; Torres, M.-J., In *Clean Solvents: Alternative Media for Chemical Reactions and Processing*; Abraham, M.; Moens, L., Eds.; ACS Symposium Series 819; American Chemical Society: Washington, DC, 2002; Vol. 3, pp 4−49.

(59) Letcher, T. M.; Deenadayalu, N. *J. Chem. Thermodyn.* **2003**, *35*, 67–76.

(60) Tong, J.; Liu, Q.-S.; Xu, W.-G.; Fang, D.-W.; Yang, J.-Z. *J. Phys. Chem. B* **2008**, *112*, 4381–4386.

(61) Fannin, A. A., Jr.; King, L. A.; Leveisky, J. A.; Wilkes, J. S. *J. Phys. Chem.* **1984**, *88*, 2609–2614.

(62) Emel'yanenko, V. N.; Verevkin, S. P.; Heintz, A.; Schick, C. *J. Phys. Chem. B* **2008**, *112*, 8095–8098.

(63) Rodriguez, H.; Brennecke, J. F. *J. Chem. Eng. Data* **2006**, *51*, 2145–2155.

(64) Ye, C.; Shreeve, J. n. M. *J. Phys. Chem. A* **2007**, *111*, 1456–1461.

(65) (a) Olivier-Bourbigou, H.; Magna, L. *J. Mol. Catal. A: Chem.* **2002**, 182. (b) Fredlake, C. P.; Crosthwaite, J. M.; Hert, D. G.; Aki, S. N. V. K.; Brennecke, J. F. *J. Chem. Eng. Data* **2004**, *49*, 954–964. (c) Tokuda, H.; Hayamizu, K.; Ishii, K.; Susan, M. A. B. H.; Watanabe, M. *J. Phys. Chem. B* **2004**, *108*, 16593–16600.

(66) Papaiconomou, N.; Yakelis, N.; Salminen, J.; Bergman, R.; Prausnitz, J. M. *J. Chem. Eng. Data* **2006**, *51*, 1389–1393.

(67) Valderrama, J. O.; Sanga, W. W.; Lazzus, J. A. *Ind. Eng. Chem. Res.* **2008**, *47*, 1318–1330.

(68) Merck ionic liquid database, http://ildb.merck.de/ionicliquids/en/startpage.html.

(69) Shanley, P.; Collin, R. L. *Acta Crystallogr.* **1961**, *14*, 79–80.

(70) Jacquemin, J.; Ge, R.; Nancarrow, P.; Rooney, D. W.; Costa Gomes, M. F.; Pádua, A. A. H.; Hardacre, C. *J. Chem. Eng. Data* **2008**, *53*, 716–726.

(71) Muhammad, A.; Mutalib, M. I. A.; Wilfred, C. D.; Murugesan, T.; Shafeeq, A. *J. Chem. Thermodyn.* **2008**, *40*, 1433–1438.

(72) Pereiro, A. B.; Tojo, E.; Rodríguez, A.; Canosa, J.; Tojo, J. *J. Chem. Thermodyn.* **2006**, *38*, 651–661.

(73) Lee, S. H.; Lee, S. B. *Chem. Commun.* **2005**, 3469–3471.

(74) Yan, T.; Burnham, C. J.; Del Pópolo, M. G.; Voth, G. A. *J. Phys. Chem. B* **2004**, *108*, 11877–11881.

(75) Repasky, M. P.; Chandrasekhar, J.; Jorgensen, W. L. *J. Comput. Chem.* **2002**, *23*, 1601–1622.

(76) Acevedo, O. *J. Phys. Chem. B*, submitted.

(77) Acevedo, O.; Jorgensen, W. L. *J. Am. Chem. Soc.* **2005**, *127*, 8829–8834.

(78) Thompson, J. D.; Cramer, C. J.; Truhlar, D. G. *J. Comput. Chem.* **2003**, *24*, 1291–1304.

(79) Hermans, J.; Wang, L. *J. Am. Chem. Soc.* **1997**, *119*, 2707–2714.

(80) D'Anna, F.; La Marca, S.; Noto, R. *J. Org. Chem.* **2008**, *73*, 3397–3403.

CT900009A